IEEE Access
Multidisciplinary ⋮ Rapid Review ⋮ Open Access Journal

Received August 14, 2020, accepted August 17, 2020, date of publication August 21, 2020, date of current version September 9, 2020.

Digital Object Identifier 10.1109/ACCESS.2020.3018597

Design Procedure of MMC-HVDC System: Comprehensive Consideration of Internal and External Dynamics

JAESIK KANG[1], (Member, IEEE), DAE-WOOK KANG[1], (Member, IEEE), JONG-PIL LEE[1], (Member, IEEE), DONG WOOK YOO[1], (Member, IEEE), AND JAE WOONG SHIM[2], (Member, IEEE)

[1]Korea Electrotechnology Research Institute, Changwon 51543, South Korea
[2]Department of Energy Engineering, Inje University, Gimhae 50834, South Korea

Corresponding author: Jae Woong Shim (jaewshim@inje.ac.kr)

This work was supported by the Korea Institute of Energy Technology Evaluation and Planning (KETEP) and the Ministry of Trade, Industry & Energy (MOTIE) of the Republic of Korea under Grant 20179310100060.

ABSTRACT This paper proposes a systematic design procedure with comprehensive consideration of the internal and external dynamics in modular multilevel converter high voltage direct current (MMC-HVDC) transmission system. Previous studies on MMC parameter selection separately deal with each specific component such as energy storage capacity for voltage ripple of sub-module (SM) capacitor, arm inductance for second harmonic circulating current reduction, maximum allowable modulation index for MMC operating condition, which considered only a single purpose. However, the parameters respond dynamically to their characteristics and interact directly with the MMC performance, power system conditions, and specific requirements. In this study, we investigate the mutual relationships between the parameters and their performance. Then, we determine the parameter values based on a proposed systematic design procedure with the desired objectives and restricted conditions, which could be cumbersome and time-consuming to approach proper and acceptable parameter values. Therefore, this study could provide engineering evaluations and insights to help MMC-HVDC system engineers and project developers in intuitive approaches regarding the design aspects of the technology requirement challenges. The efficacy and accuracy of the analysis and design method for the MMC-HVDC system parameters were validated by PSCAD/EMTDC time-domain simulation and real-time digital simulation with hardware-in-loop system.

INDEX TERMS Arm inductance, capacitance, design, high-voltage direct current (HVDC), HILS, modular multilevel converter (MMC), modulation index, PSCAD/EMTDC, RTDS, sub-module (SM).

I. INTRODUCTION

Modular multilevel converter (MMC) application has been widely adopted by power utilities in recent years, as its inherent attributes bring clear advantages compared with two-level voltage-sourced converter (VSC) due to reduced losses and footprint of mega-scale applications such as high voltage direct current (HVDC) transmission system, flexible alternating current transmission systems (FACTS), medium voltage DC system, and motor drives, introduced in [1]–[10]. Previous research for MMC applications attempted to achieve stable performance, control, design, and its operation as a grid-tied converter [11]–[21]. Among these key studies, the methodology for parameter determination is an important subject to achieve enhanced MMC-HVDC systems. The purpose of designing the parameters in previous studies was to make MMC capable for steady-state operation, allowing it an improved ability through goal-oriented design solutions based on the precise analysis of internal dynamics. The previous design philosophy could lack a system integration and cause an inaccuracy between an anticipated performance and a required specification of MMC-HVDC system, since complicated interaction exists between the internal and external parameters due to large power system interconnection. Therefore, a comprehensive analysis of the parameter relationships and a systematic process should be established to improve the

The associate editor coordinating the review of this manuscript and approving it for publication was Dwarkadas Pralhaddas Kothari.

MMC-HVDC system without adverse impacts on bulk power system.

In general, there are main components in MMC development such as the energy storage capacity for capacitor voltage ripples and arm inductance for second harmonic circulating current reduction. The most important part of MMC design is the determination of sub-module (SM) capacitance. MMC utilizes the stored energy in SM capacitors, which are required in a larger number than conventional two-level VSC. Therefore, it must be designed carefully to maintain its performance. The method of estimating the energy storage capacity was introduced when MMC was proposed by Marquardt [22]. Similarly, calculation methods were developed in detail in some studies and used to calculate SM capacitance [23]–[25]. In [26]–[29], a design methodology considering capacitor voltage ripple according to the operating point was introduced based on the same approach. References [30]–[33] used simple equations based on the results empirically derived in [26]. [34] adopted a design method based on the detailed analysis of the MPPF-based capacitor in terms of aging and voltage ripple. Previous studies on energy storage capacity focused on attempting to design an available specification. However, the parameter should be comprehensively analyzed and then determined considering requirements and limitations due to the connected power system condition.

Arm inductance could be considered for an inevitable second harmonic circulating current, a sudden fault current, and unwanted resonance in MMC. To reduce the second harmonic circulating current, the design method of arm inductor as a harmonic filter was introduced [35]–[37]. This method is less preferable in terms of harmonic stability than a proper control scheme, which indicates that there is a disadvantage in the necessary arm resistance even if a virtual arm resistance is available to secure harmonic stability [38]. Hence, it is assumed that it is not used in actual MMC-HVDC systems to avoid undesired adverse impacts from a stability point of view. Reference [31] showed a design method through the analysis of resonance generation area between SM capacitance and arm inductance. This is the method to avoid areas where the resonance may occur at twice the fundamental frequency. Reference [39] introduced a method for suppressing the second harmonic circulating current generated by the capacitor voltage ripple and reducing the fault current rise rate by analyzing the internal dynamics of MMC. However, since the method is not considered for the circulating current suppression control (CCSC) scheme that eliminates the second harmonic circulating current, more careful selection with MMC auxiliary control effect is necessary by multi-faceted judgment.

In addition to the above parameters, the modulation index for MMC-HVDC system was analyzed in [40]–[42]. This study determines the PQ capability which is the basis of VSC principle. In general, the modulation index is determined according to the operating point of the VSC, and the modulation index equal to 1 is ideal without 3rd harmonic injection strategy. However, if the compensation voltage considering the circulating current introduced above is synthesized on the original reference voltage, the modulation index will be less than one. Therefore, the MMC-HVDC developer should consider the maximum modulation index to meet the PQ requirements accounting for SM capacitance and arm inductance in the initial design. For the MMC-HVDC system design concerning SM capacitance, the arm inductance, and modulation index mentioned above, the design and analysis were carried out in [43], [44]. However, operating conditions of MMC may be changed by parameters owing to the influence of the control techniques required for MMC conditions. Hence, MMC-HVDC system design should be based on a comprehensive analysis of the impact of additional control techniques of MMC such as voltage balancing control with sorting algorithm and CCSC [45]–[56]. Furthermore, voltage and current at AC and DC sides of the MMC-HVDC system should be selected in various ways according to the design of the previously introduced components as well as MMC voltage level considering connected power system conditions. Therefore, in this study, a systematic design procedure of MMC-HVDC system parameters is established regarding their characteristics for comprehensive and approachable development.

The remainder of this paper is organized as follows: Section II includes a brief overview of the internal dynamics of MMC. In Section III, the relationships between the parameters and the performance are properly investigated, and the MMC-HVDC system parameters determination methodology is proposed in Section IV. Finally, PSCAD/EMTDC time-domain simulation results for verifying the determined parameters are shown in Section V, followed by the conclusion in Sections VI.

II. BASIC MMC DYNAMICS FOR PARAMETERS

Fig. 1 indicates the configuration of MMC. V_{dc} is the DC link voltage between positive and negative pole in HVDC system and I_{dc} is the DC current. V_c is capacitor voltage and i_c is the capacitor current flowing into each individual capacitor. i_{arm} is the arm current consisting of upper (i_{armp}) and lower (i_{armn}) arm currents including AC (i_{sj}) and circulating currents (i_{cir}) (phase $j = a, b, c$, and the subscript p denotes the upper arm and n denotes the lower arm), which can be expressed as [14]:

$$i_{armp} = \frac{i_s}{2} + i_{cir}. \tag{1}$$

$$i_{armn} = -\frac{i_s}{2} + i_{cir}. \tag{2}$$

$$i_{cir} = \frac{i_{armp} + i_{armn}}{2} = \frac{i_{dc}}{3} + i_{2f}. \tag{3}$$

where i_{2f} is second harmonic circulating current. V_{sm} is terminal voltage generated from SM consisting of two-level half-bridge converter depicted in Fig. 1. According to [14], MMC is featured by the following equations

$$V_{tj} = e_j - \frac{R_{arm}}{2} i_{sj} - \frac{L_{arm}}{2} \frac{di_{sj}}{dt}. \tag{4}$$

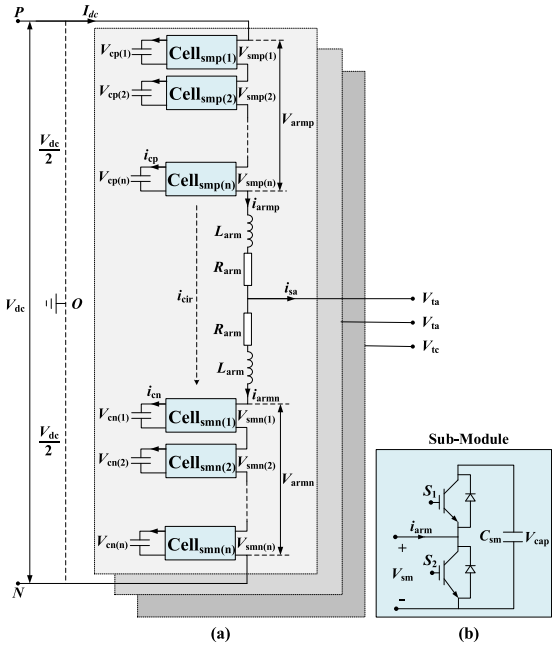

FIGURE 1. Schematics of (a) the modular multilevel converter and (b) half-bridge sub-module (SM).

$$L_{\text{arm}}\frac{di_{\text{sj}}}{dt}+R_{\text{arm}}i_{\text{sj}}=\frac{V_{\text{dc}}}{2}-\frac{V_{\text{armp}}+V_{\text{armn}}}{2}. \tag{5}$$

where e_{j} in (4) is the inner EMF generated in phase j and desired inner voltage as a sinusoidal waveform, which can be expressed as:

$$e_{\text{j}}=\frac{V_{\text{armn}}-V_{\text{armp}}}{2}=\frac{m}{2}\cdot V_{\text{dc}}\cdot\sin(\omega_0 t). \tag{6}$$

The reference arm voltage could be defined from the above analysis as follows:

$$V_{\text{pref}}=\frac{V_{\text{dc}}}{2}-e_{\text{j}}. \tag{7}$$

$$V_{\text{nref}}=\frac{V_{\text{dc}}}{2}+e_{\text{j}}. \tag{8}$$

III. PARAMETER ANALYSIS OF MMC-HVDC SYSTEM

A. EXTERNAL PARAMETERS OF MMC-HVDC SYSTEM

The MMC parameters to be considered are listed in Table 1 for accomplishing a stable operation and control of MMC-HVDC system in Fig. 2. Active power (P_{s}) plays a key role in MMC-HVDC planning process as pre-determined variables, and is naturally determined by line impedance as well as angle differences between grid-side voltage and MMC-side voltage. Reactive power (Q_{s}) is also highly related to the modulation signal, which factors are influenced by internal and external conditions; thus, we will provide the guideline of parameter determination in this research. Reactive power (Q_{s}) value should be determined due to the voltage deviation and this kind of reactive power should be determined by power system study. In other words, active power is determined with transmission power capacity and the design specification of reactive power can be determined, based on power system study such as simulation.

Although the primary voltage of transformer is a predetermined parameter on the basis of grid-side rating, the secondary voltage should be properly determined and thoroughly studied, as it determines the characteristics of PQ capability directly associated with DC voltage and current. The secondary voltage also affects the modulation index, the number of SMs, SM capacitance, arm current, and arm inductance, and those factors should be considered for reliability, system loss, and stability requirements.

In sum, internal dynamics and parameters of MMC heavily rely on secondary voltage of AC side.

B. INTERNAL PARAMETERS OF MMC-HVDC SYSTEM

1) DC VOLTAGE AND CURRENT

In Table 1, the main parameters for MMC operation are shown. DC voltage and current are economic variables in relation to active power assuming that DC power is equal to AC power and additional power losses due to passive elements and power conversion. The DC voltage is inversely proportional to DC current for constant DC power, and it relates to switching device rating. Therefore, both parameters could be considered in terms of economic requirements. Especially, DC voltage highly relates to modulation index because MMC terminal voltage (V_{t}) is determined by $(m \cdot V_{\text{dc}})/2$ which affects PQ capability. The DC current should be considered with the DC cable rating that is related to the cost of an important part of HVDC system where economical requirements have to be considered.

2) THE NUMBER OF SMs AND REDUNDANT SMs

The number of SMs relates to a blocking capability of a switching device for individual SM voltage (V_{sm}) with a determined DC voltage. It is an economic consideration variable that can be determined within a range to meet the DC link voltage and the rating of the switching device.

The number of redundant SMs depends on the redundancy methods [57]. For a passive mode (cold reserve state) for the redundancy, the number of redundant SMs is a variable independent of the MMC-HVDC system operation in which economics and reliability are to be considered together. Thus, it can be determined through optimization to enhance the MMC-HVDC system reliability after the system variables are determined. Otherwise, an active mode (hot spinning reserve state) has an effect on capacitor voltage ripple and switching frequency depending on power losses [57]. In the case of the active mode, the number of redundant SMs should be considered with reliability and economical requirement as well as system loss evaluation.

3) ARM INDUCTANCE

Arm inductor should be designed according to three factors. These are: to reduce the second harmonic circulating current

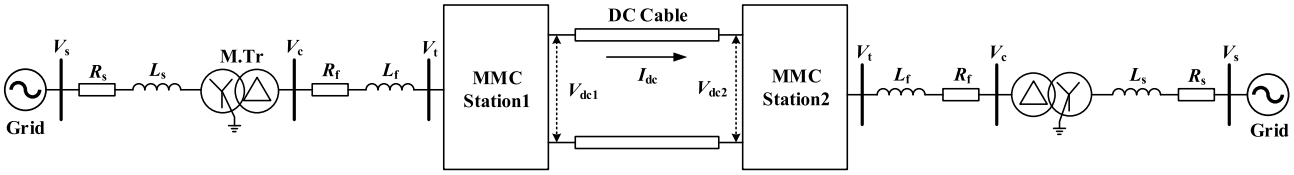

FIGURE 2. Schematic of MMC-HVDC transmission system.

TABLE 1. The key parameters of MMC-HVDC transmission system.

Parameters	Type	Objectives	Interaction factors	Deterministic methods
Active power (P_s)	Known(pre-defined) /Power system desired value	Reliability, economical and policy requirements (cost minimization and revenue maximization), auxiliary control	AC voltage, DC voltage, DC current, line impedance, modulation index	Depending on power system planning process-feasibility study with various network case study (planning considerations)
Reactive power (Q_s)	Known(pre-defined) /Power system desired value	Dynamic reactive support and dynamic control(voltage control)	AC voltage, DC voltage, DC current, line and arm inductance, modulation index	Depending on reactive power support requirement
Transformer voltage @ grid side (V_s)	Known variable	To meet a connected point	Power losses, economical requirement, fault current and SCR	Already determined value
Transformer voltage @ valve side (V_c)	Decision variable	Economical requirement	PQ capability, economic, fault current, DC voltage	Depending on available PQ requirements related with DC voltage
DC voltage (V_{dc})	Decision variable	To meet economical requirement, insulation and IGBT rating	Secondary voltage, modulation index, IGBT blocking voltage, No. of SMs	Active power requirement, cost-optimization, and IGBT rating
DC current (I_{dc})	Decision variable	To meet the economical requirements, capacity and IGBT rating	Modulation index, arm current and IGBT rating	Consideration of IGBT and DC cable rating
No. of SMs (N_0)	Decision variable	Communication constraint, harmonics (power quality) and filtering equipment	DC voltage and individual SM voltage	Consideration of DC voltage and IGBT rating
No. of redundant SMs (N_r)	Not defined	Reliability and economical requirement	Switching frequency, losses, and capacitor voltage ripple	Reliability optimization and cost-optimization
Arm inductance (L_{arm})	Decision variable	Fault current rising rate, and second harmonic current reduction	Apparent power, power factor, capacitance and second harmonic current	Reactive power loss, second harmonic current consideration and DC fault rising rate
SM capacitance (C_{sm})	Decision variable	To meet MMC stable operation (above minimum energy storage capacity)	Apparent power, power factor, arm inductance, capacitor voltage ripple and modulation index	Required energy storage capacity and voltage ripple
Maximum allowable modulation index (m_{max})	Decision variable	To prevent overloaded operation (maximum limitation for MMC capability)	Apparent power at operating point, PQ capability and compensation voltage	MMC maximum available voltage with m in addition to compensation voltage from CCSC
Individual SM voltage (V_{sm})	Decision variable	To meet semi-conductor rating	IGBT blocking voltage	Cost optimization
Arm current (I_{arm})	Decision variable	To meet semi-conductor rating	k associated with arm current over DC current and DC voltage	Cost optimization
Capacitor voltage ripple factor (k_{max})	Not defined	To be reliable (capacitor ageing and insulation)	Capacitance and PQ capability	Reliability and system losses
Switching frequency (f_{sw})	Decision variable	To balance performance and cost	Power conversion efficiency, power quality and voltage ripple	System loss and performance
PQ Capability (PQ_{cap})	Not defined	To define allowable range in MMC capability	AC voltage, DC voltage, line arm inductance, voltage ripple and SCR	PQ capability equation

* m = modulation index (rate of MMC generated voltage over DC voltage)
* k = modulation index (rate of arm current over DC current)

flowing inside the MMC, the fault current rise rate and to consider the reactive power consumption while avoiding resonance in the MMC circuit. Particularly, since arm inductor is related to CCSC strategy, it should be designed for stability and reactive power loss of MMC-HVDC system. For CCSC, arm inductor only needs to consider reactive power loss and stability, and when CCSC is disabled, second harmonic circulating current reduction studied in many previous studies is the main purpose.

4) SM CAPACITANCE, VOLTAGE RIPPLE, SWITCHING FREQUENCY

Energy storage capacity is a fundamental parameter that allows MMC to operate in a stable region. SM capacitance is an important parameter related to voltage ripple that affects the lifespan of SM capacitor. Hence, it should be managed to be generated within the limitation that designates voltage ripple factor (k_{max}). The voltage ripple management is related to the switching frequency (f_{sw}), which influences the power

conversion loss and power quality. As a result, the energy storage capacity should be designed considering reliability and economical requirements while guaranteeing minimum MMC operating conditions [58].

5) PQ CAPABILITY

The modulation index of conventional VSC is related to the operating point for desired active and reactive powers. Furthermore, MMC has additional factors affecting the modulation index, which are the compensation signal generated due to the control to reduce the second harmonic circulating current and additional reactive power consumption by the arm inductor. In this paper, the physical factors discussed in the previous research are not considered because their influences could be negligible [40], [41].

6) ARM CURRENT

Arm current is related to the rating of the switching device and includes AC and DC currents as shown in (1)-(3). When the above mentioned main parameters are determined, it can be selected by the modulation index (k) of AC current over DC current. In this study, even though the second harmonic circulating current increases the peak value of the arm current, it is assumed that it becomes zero by CCSC strategy.

IV. DESIGN OF MMC-HVDC TRANSMISSION SYSTEM

A. CONSIDERATIONS OF DESIGN

MMC parameter should be designed with the trade-off relationship between cost-effectiveness and system reliability. In this study, however, a design method is developed from the performance perspective of MMC-HVDC system except for economical and reliable factors that are assumed as variables being optimized from manufacturers. In addition, it is assumed that the desired active and reactive power values depend on possible HVDC applications to current power systems, and no overload capability of the whole equipment is applied.

The initial MMC-HVDC design phase defines the P-Q rated values and AC voltage to be connected through the grid planning process. The internal and external parameters for MMC design should be calculated only with the minimum parameters obtained from the system planning. In this study, a systematic design process is proposed for obtaining the parameters introduced in Table 1. For reliability and economical requirement-based design, the optimization process is applied independently with the proposed methodology and is not considered in this paper.

B. DESIGN PROCEDURE

Fig. 3 indicates the flow chart of MMC design procedure. The design methodology proposed in this paper is as follows.

1) PREREQUISITE VALUES (P_s, Q_s, P_{dc}, V_s)

Active and reactive power and AC voltage at the grid connection point are determined at the grid planning stage. These

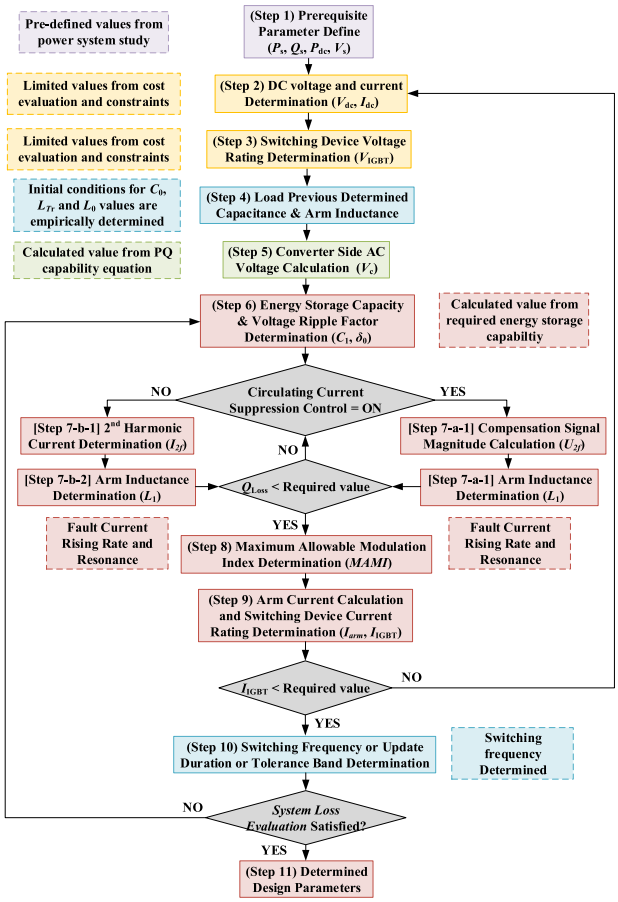

FIGURE 3. Flow chart of design iteration procedure.

are pre-defined parameters before the determination process of the main parameter. These parameters are provided after the power system study completion.

2) DC VOLTAGE AND CURRENT (V_{dc}, I_{dc})

In general, DC voltage could be determined by a loss-cost optimization, and DC current could be determined by considering the cable cost corresponding to the long distance. Once DC voltage is optimized according to the HVDC transmission length, other MMC parameters could follow the design process provided in Fig. 3. In this study, it begins by selecting the DC voltage optimized from a cost assumption as the maximum value in Fig. 4, and redefined considering the

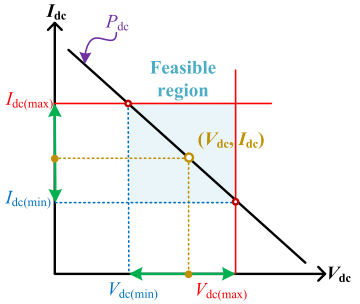

FIGURE 4. DC voltage and current determination method.

rated current of the switching device as shown in the Step 9 of Fig. 3. As shown in Fig. 4, the DC voltage and current to meet the required DC power are inversely proportional. Hence, as the DC voltage is fixed, the DC current could be calculated, and the entire design process would be iterated while identifying the required conditions.

3) INDIVIDUAL SUB-MODULE VOLTAGE (V_{IGBT}, V_{sm})

The variable of individual SM voltage determines the number of SMs for DC voltage of MMC which is related to the voltage rating of the switching device thereby individual SM voltage magnitude could be applied as an optimization target with the economic evaluation. In this paper, we suggest the recommended voltage utilization value (λ_v) of 60 % over the rating of the switching device is used in (9) and specifications suitable for the ratings of commercial products are adopted.

$$V_{dc} = N_0 \cdot V_{sm} = N_0 \cdot \lambda_v \cdot V_{IGBT}. \tag{9}$$

where V_{dc} is DC voltage of MMC, N_0 is the number of SMs, V_{sm} is the nominal voltage of SM, λ_v is the voltage utilization factor, and V_{IGBT} is the voltage rating of IGBT.

4) SETTING INITIAL PARAMETER AND UPDATING PREVIOUSLY DETERMINED PARAMETERS (L_0, C_0, L_{tr})

To obtain the secondary voltage of the main transformer being determined in next section (Step 5), the necessary parameters should be estimated as an initial parameter. A primitive energy storage capacity could be obtained as follows [31],

$$C_0 = \frac{N_0 \cdot EP_0 \cdot S_n}{3 \cdot V_{dc}^2}. \tag{10}$$

where C_0 is initial parameter of SM capacitor which would be updated during the process, EP_0 is energy per power ratio (20∼50 [kJ/MVA]) for the capacitance that meets the normal operation of MMC [26], [30]–[33], [57], and S_n is the apparent power based on $V_{dc}I_{dc}/cos(\varphi)$.

A temporary arm inductance value could be obtained by assuming that the second harmonic circulating current (I_{2f}) is a specific value, as follows [39],

$$L_0 = \frac{1}{8 \cdot \omega_0^2 \cdot C_0 \cdot V_{sm}} \cdot \left(\frac{S_n}{3 \cdot I_{2f}} + V_{dc} \right). \tag{11}$$

where L_0 is initial parameter of arm inductance which would be updated during the process, I_{2f} is second harmonic circulating current, and ω_0 is the nominal angular frequency.

To specify the second harmonic circulating current value for the variable, X_{Lpu} could be empirically selected to an approximate 0.1 [p.u] as a desirable value due to reactive power consumption in the arm reactance [32]. From (11) with (9), (10), (12) and (13), per unit value of arm inductance could be defined as (14):

$$Z_{base} = \frac{V_{LL}^2}{S_n}. \tag{12}$$

$$V_{LL} = m \frac{V_{dc}}{2} \sqrt{\frac{3}{2}}. \tag{13}$$

$$X_{Lpu} = \frac{1}{\omega_0 \cdot EP_0} \left(\frac{I_{dc}}{3\cos(\varphi) \cdot I_{2f}} + 1 \right). \tag{14}$$

where Z_{base} is the impedance base, V_{LL} is the line to line AC voltage, and m is the modulation index.

Therefore, the specific second harmonic circulating current (I_{2f}) could be calculated with assuming that the per unit value of X_{Lpu} is 0.1 [p.u] and modulation index is 1 in (12) and (13) for (14) as follows,

$$I_{2f} = \frac{I_{dc}}{3\cos(\varphi) \cdot (X_{Lpu} \cdot \omega_0 \cdot EP_0 - 1)}. \tag{15}$$

The initial parameter of (I_{2f}) is determined with the brief value. Thus the value should be recalculated to find a more appropriate value for an important role of PQ capability, stability and fault current rising limitation. Leakage inductance (L_{tr}) of the main transformer can be determined by the transformer manufacturer as in [43]. In this study, however, we adopted the general value used in [26].

5) CONVERTER SIDE AC VOLTAGE (Secondary VOLTAGE, V_c)

Secondary voltage of the main transformer should be determined within a restricted range that meets an operable modulation index of MMC while providing the required active and reactive power. Using the PQ capability curve formula, a maximum acceptable MMC voltage should be selected to define the secondary voltage. The formula for PQ capability is as follows,

$$P_s^2 + \left(Q_s + \frac{V_s^2}{X_{eq}} \right)^2 = \left(\frac{V_s \cdot V_c}{X_{eq}} \right)^2. \tag{16}$$

where $X_{eq} = \omega L_{tr} + \omega L_f + \omega L_{arm}/2$ as depicted in Fig. 1 and 2.

In this study, however, we assumed that $L_f = 0$ because the interface transformer is installed close to the terminal of MMC, thereby the line impedance between them is negligible, and V_c is equal to V_t. Moreover, since the primary voltage of the transformer has an allowable operating range regulated by the connected grid code, the secondary voltage has also the regulated voltage range. As a result, when MMC performs only pure reactive power compensation (STATCOM mode), which has a maximum voltage while supplying Q_{max} within the rated power of MMC, the secondary voltage could range in the regulated AC voltage from 0.95 to 1.05 [p.u] assuming that the grid code is an arbitrary value. In (16) with the conditions of $P_s = 0$, Q_{max} and $V_{spu} = 1.05$ [p.u], secondary voltage could be calculated as follows.

$$V_{cpu} = \frac{X_{eqpu} \cdot Q_{maxpu}}{V_{spu}} + V_{spu}. \tag{17}$$

where V_{cpu} is the converter side AC voltage, X_{eqpu} is the equivalent total reactance, Q_{maxpu} is the maximum reactive power requirement and V_{spu} is the grid side AC voltage at per unit value, respectively.

When the secondary voltage is considered with modulation index, it depends on the DC voltage that provides the AC terminal voltage of MMC and summed by individual SM

voltage multiplying the number of activated SMs. Therefore, MMC DC voltage could be as follow,

$$V_{\mathrm{dc}} = \sum_{j=0}^{N_0} V_{\mathrm{cap}j} = \sum_{j=0}^{N_0} (V_{\mathrm{sm}j} + \Delta V_{\mathrm{ripple}j}). \tag{18}$$

where k_{max} is the voltage ripple factor and $\Delta V_{\mathrm{ripple}}$ is $k_{\mathrm{max}} \cdot V_{\mathrm{sm}}$. From (18), minimum DC voltage due to k_{min} that is $k_{\mathrm{max}} = -k_{\mathrm{min}}$, is as follows [26],

$$V_{\mathrm{dcmin}} = V_{\mathrm{dc}}(1 - k_{\mathrm{max}}). \tag{19}$$

Since the value obtained in (17) should be 1 [p.u] under the condition of (19), the maximum converter side AC voltage for line-to-line RMS value is as follows with (13),

$$V_{\mathrm{c}} = \frac{V_{\mathrm{dcmin}}}{2 \cdot V_{\mathrm{cpu}}} \sqrt{\frac{3}{2}}. \tag{20}$$

6) ENERGY STORAGE CAPACITY (SM CAPACITANCE, C_{sm})

Energy storage capacity of SM could be adjusted with the previously determined parameters and a desirable voltage ripple factor based on a detailed analysis through (40) of [26]. The initial SM capacitance (C_0) is in the range of a stable operating condition due to the particularly conservative value. Moreover, the voltage ripple is determined by the natural response of the initially designed values. However, the CCSC control algorithm could reduce the voltage ripple, which affects the internal dynamics of MMC. Conversely, a voltage balancing algorithm for the voltage ripple could aggravate the voltage ripple, which would cause a forced ripple. Therefore, the required voltage ripple factor is associated with switching frequency depending on the MMC system loss, which should be examined with a specific switching principle adopted by the MMC developer and designed with the loss evaluation in the design step (Step 10) of the design process [46], [48], [49], [59], [60]. In this paper, the SM capacitance is only validated for analysis in whether stable operating point or not under the full-sorting algorithm.

7) ARM INDUCTANCE (L_{arm})

In case circulating current suppression control (CCSC) is disabled, arm inductance is determined by selecting the second harmonic circulating current mentioned in Step 4 of the design procedure. The CCSC, however, is conventionally enabled for MMC-HVDC transmission system. Arm inductance depends on whether the CCSC activates or deactivates, which should be considered.

a: CASE I WITHOUT CIRCULATION CURRENT SUPPRESSION CONTROL

- (a-1) second harmonic circulating current calculation ($I_{2\mathrm{f}}$): the $I_{2\mathrm{f}}$ could be calculated by (15) with a redefined energy per power ratio (EP_0) through the SM capacitance validated from previous step.
- (a-2) Arm inductance calculation (L_{arm}): Arm inductance could be calculated by (11), and it should be investigated if the value avoided the resonance point through [31], [39], [44].

b: CASE II WITH CIRCULATION CURRENT SUPPRESSION CONTROL

- (b-1) Compensation voltage calculation ($U_{2\mathrm{f}}$): Equation (11) provides arm inductance determination method without CCSC, thereby the resulting second harmonic voltage across the arm inductor is equal to (32) in [39] assuming that (24) and (25) in [39] include the second harmonic current component in arm current. However, with the CCSC algorithm, the second harmonic circulating current term should be removed in (26) in [39]. Thus the equation should be derived without the second harmonic term, therefore, as follows,

$$U_{2\mathrm{f}} = \frac{S_{\mathrm{n}}}{6 \cdot \omega_0 \cdot C_0 \cdot V_{\mathrm{sm}}}. \tag{21}$$

- (b-2) Arm inductance determination (L_{arm}): Arm inductance with the CCSC could be designed regarding fault current rise rate for gate turn-off delay while a resonance problem is investigated [31], [39], [44], because the second harmonic circulating current is negligible at this time.

8) MAXIMUM ALLOWABLE MODULATION INDEX (MAMI)

The initial maximum allowable modulation index (m_{max0}) is based on (20) for the secondary voltage in the case without CCSC strategy. However, for the compensation voltage signal (m_{U2f}) obtained (21) owing to voltage ripple generated by SM capacitor natural dynamics, the MAMI could be acquired by

$$m_{\mathrm{max}} = m_{\mathrm{max0}} - m_{\mathrm{U2f}}. \tag{22}$$

where m_{max0} is the MAMI without CCSC and m_{U2f} is the compensation signal index. In this study, 3rd harmonic injection strategy is not considered.

9) ARM CURRENT AND IGBT CURRENT (I_{arm}, I_{IGBT})

The current rating of switching device (I_{IGBT}) has also a current utilization factor (λ_i) such as the individual SM voltage determination in (9) due to a thermal consideration, as follows,

$$I_{\mathrm{IGBT}} = \lambda_i \cdot I_{\mathrm{arm}}. \tag{23}$$

From (1) and (2) for arm currents (I_{arm}), a ratio of AC and DC currents (k) is as follows,

$$k = \frac{3I_{\mathrm{s}}}{2I_{\mathrm{dc}}}. \tag{24}$$

Assuming that the DC and AC powers are equal with a lossless system as follows,

$$P_{\mathrm{dc}} = V_{\mathrm{dc}} \cdot I_{\mathrm{dc}} = \sqrt{3} \cdot V_{\mathrm{s}} \cdot I_{\mathrm{s}} \cdot \cos(\varphi) = P_{\mathrm{s}}. \tag{25}$$

From (13) and (24) in (25), the following equation is derived,

$$k \cdot m \cdot \cos(\varphi) = 2. \tag{26}$$

From (1), (2), (24) and (26), arm current is as follows,

$$I_{\text{arm}} = \frac{I_{\text{dc}}}{3} \cdot (k+1) = \frac{I_{\text{dc}}}{3} \cdot \left(\frac{2}{m \cdot \cos(\varphi)} + 1 \right). \quad (27)$$

For ease of the device current rating, γ_0 is used as the MMC arm current rating factor and with minimum value of 1 in case that $m = 1$ and $\varphi = 0$, as follows,

$$\gamma_0 = \frac{1}{3} \cdot \left(\frac{2}{m \cdot \cos(\varphi)} + 1 \right) \geq 1. \quad (28)$$

However, m and φ depend on operating point from (16). Therefore, when the MMC-HVDC system operates to unity power factor(assuming the condition of PQ curve linear ramp rate), the modulation index that could be obtained in step (Step 5) is the smallest. The operating angle could be calculated under this condition, as follows,

$$\varphi = \arcsin \left(P_{\text{s}} \cdot \frac{X_{\text{eq}}}{V_{\text{s}} \cdot V_{\text{c}}} \right). \quad (29)$$

From (27) and (28), final arm current is as follows,

$$I_{\text{arm}} = \gamma_0 \cdot I_{\text{dc}}. \quad (30)$$

As a result, the current rating of switching device could be determined considering specific products from many semi-conductor manufacturers, and inspected in terms of economical aspect. From (28) and (30), final IGBT current is as follows,

$$I_{\text{IGBT}} = \lambda_i \cdot \gamma_0 \cdot I_{\text{dc}}. \quad (31)$$

10) SYSTEM LOSS EVALUATION

System losses consists of the power losses on passive elements (interface transformers, lines, connection points, DC cables) and power conversion elements (active device). The system loss evaluation in this paper focuses on switching loss highly related to the SM capacitance with the voltage ripple factor that limits the switching frequency and various capacitor voltage sorting algorithms [59], [60]. The voltage fluctuation of the SM capacitor is determined by a natural voltage ripple and a forced voltage ripple. When energy storage capacity is obtained from the design step (Step 6), the voltage ripple factor (k_{max}) is considered as a purely natural voltage ripple. Owing to the characteristics of MMC, however, voltage ripple is additionally generated by various capacitor voltage sorting techniques, which denote forced ripples generated by external factors [40]. Based on the characteristics, the active mode redundancy method could inversely reduce the capacitor voltage ripple [57], and thus the system loss evaluation should be investigated with the various relationship in terms of reliability and economical requirement. Therefore, for the system loss, the voltage ripple is determined according to the SM capacitance, the sorting algorithms, and redundancy methods. Finally, the switching frequency that can satisfy the system loss can be determined. Since this study was extensively scrutinized by previous studies [57], [59], [60], only the verification is conducted with an assumption that a required MMC-HVDC system adopts the passive mode redundancy method in this paper.

11) FINAL DESIGN PARAMETERS VERIFICATION AND DETERMINATION

The determined parameters were validated by PSCAD/EMTDC simulation, which is shown in the next section.

V. VALIDATION OF DESIGN PARAMETERS FOR MMC-HVDC TRANSMISSION SYSTEM

A. PSCAD/EMTDC SIMULATION RESULTS

For the MMC-HVDC system parameters, PSCAD/EMTDC simulation with a time step, $1/(2\pi f_0 m N_0)$, is based on [61], [62], allowing for accuracy of interacting between the HVDC transmission system and MMC performance. Furthermore, MMC control is focused on direct modulation associated with the dq-framed CCSC method [46]. This paper confines the parameters offered in Table 1 that provide the required prerequisite variables and necessary parameters for MMC-HVDC. The determined parameters are shown except for the complete design procedure because detailed economical and reliability evaluations are required to finalize the optimized MMC-HVDC system parameters. The economical requirements and reliability are out of the scope of this study. However, this research provides a design approach to expand an insight regarding the entire MMC-HVDC transmission systems.

Table 2 indicates that necessary parameters for the MMC-HVDC system are determined by the proposed design procedure. Except for the economical requirements of the DC voltage and the switching device, it begins that V_{dc} is fixed to ± 120 kV. As shown in (a) of Fig. 9, the MMC-HVDC system has an operating point that the active and reactive power are 200 MW and 60 MVar at the required normal operation as shown in (a) and (b) of Fig. 5, when the reference commands are 1.0 and 1.5 s, respectively. Under these conditions, AC voltage at the grid side is 154 kV and DC current is 833.3 A. The ratings of switching devices for commercial product is 4 kV. However, the individual SM voltage is 2.4 kV considering a recommended voltage utilization factor (60%) as shown in (f) of Fig. 5. Hence, the number of SMs is 100 without redundancy. For initial energy storage capacity, 50.0 [kJ/MVA] is adopted and the SM capacitance is 6000 μF which is not considered for voltage ripple limitation. As a result, voltage ripple is 7.5% when arm inductance, which is X_{Lpu} is 0.1 [p.u] and a specific $I_{2\text{f}}$ is 300 A obtained from (15), is the main role of reducing the second harmonic circulating current component without the CCSC. The second harmonic circulating current is injected into the arm current thereby the arm current is distorted as depicted in (h) of Fig. 5. Based on the initial parameters, the temporary secondary voltage at the valve side is calculated as 128.317 kV through (15). The final reference signal and calculated modulation signal are well matched and the valve side voltage is generated within the defined voltage level.

Considering the CCSC strategy, the compensation voltage should be defined when the maximum reactive power support, in shown (b) of Fig. 9 is enabled as a STATCOM

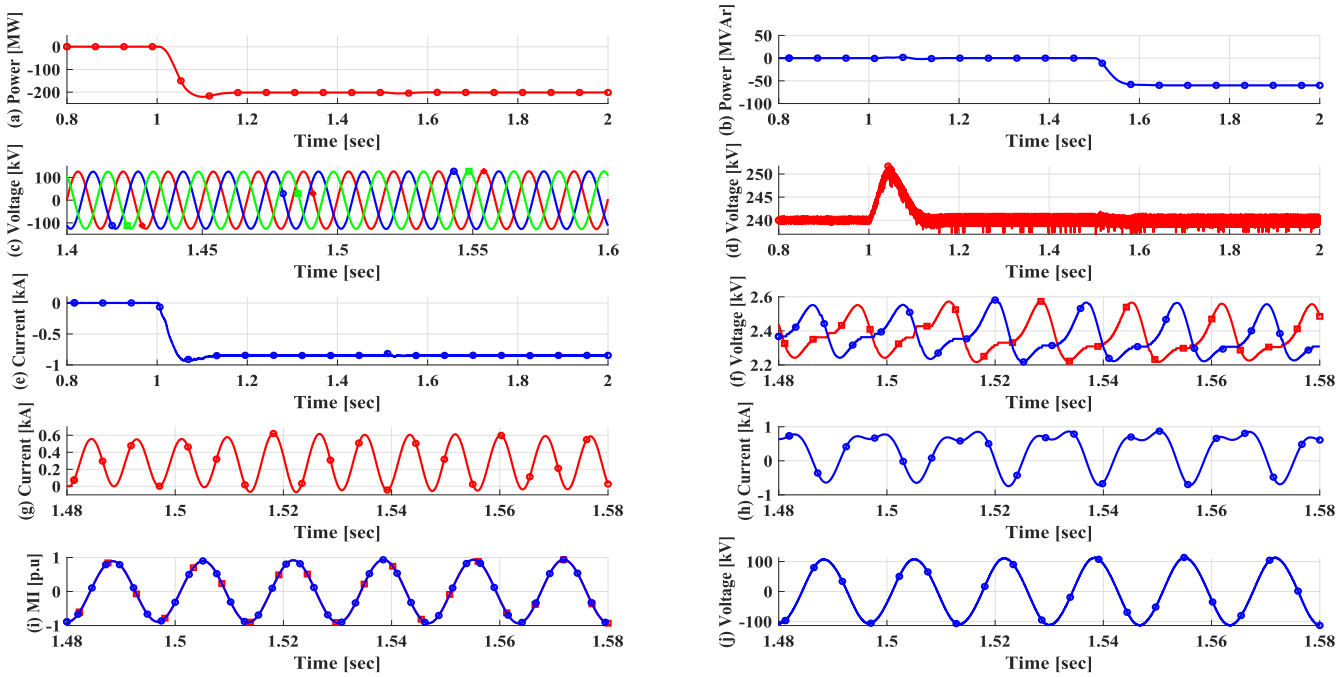

FIGURE 5. Simulation results: (a) active power, (b) reactive power, (c) AC voltage, (d) DC voltage, (e) DC current, (f) capacitor voltage, (g) circulating current, (h) arm current, (i) modulation signal and (j) converter voltage.

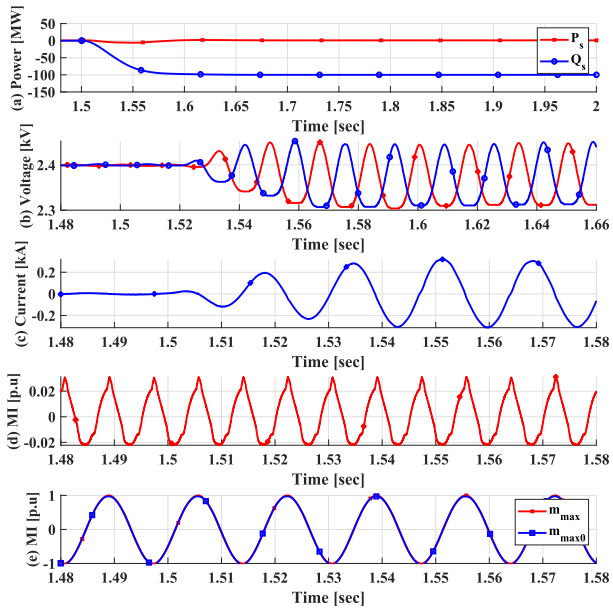

FIGURE 6. Simulation results: (a) active and reactive power, (b) capacitor voltage, (c) arm current, (d) compensation signal and (e) modulation signal.

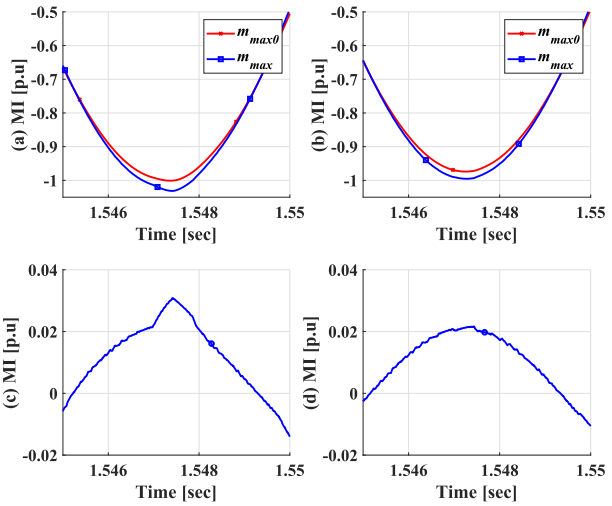

FIGURE 7. Simulation results: (a) modulation signal without MAMI and (b) modulation signal with MAMI, (c) compensation signal without MAMI and (d) compensation signal with MAMI.

mode at 1.5s as shown in (a) of Fig. 6. The arm current has only fundamental frequency component due to the CCSC as shown in (c) of Fig. 6. However, the reference signal plus the compensation signal that is 0.025 obtained from (21), shown in (c) of Fig. 7, is over-modulated as shown in (a) of Fig. 7. Therefore, the valve side voltage considering the MAMI should be re-defined through (20) and (22). The final valve side voltage is updated from 128.317 kV to 124.94 kV considering the MAMI due to the compensation voltage. As shown in (b) of Fig. 7, the maximum allowable modulation index is within the available range. With the CCSC strategy, the initial arm inductance could be validated in terms of undesirable resonance phenomenon through [44], which is 380.17 rad/s within the safe region. Finally, the arm current depicted in Fig.(8) is well matched compared with the value obtained from (30), where the γ_0 is 1.169, the I_{dc} is 833.3 A, and hence the I_{arm} is 973.9 A.

TABLE 2. MMC-HVDC system parameters for PSCAD/EMTDC simulation.

Parameter	Value	Description
Active power (P_s)	200 MW	Required value at steady state
Reactive power (Q_s)	60 MVar	Desired value for grid support
STATCOM mode	$\pm$100 MVar	Desired value (Q_{max} is capacitive mode)
System frequency	60 Hz	Fundamental frequency
Transformer voltage @ grid side (V_s)	154 kV	Defined value
Transformer voltage @ valve side (V_c)	125 kV	For stable operation of MMC from Eq.(20) and Eq.(22)
DC voltage (V_{dc})	$\pm$120 kV	Estimated value without economical requirement
DC current (I_{dc})	833.3 A	No consideration of DC cable distance
No. of SMs (N_0)	100 ea	From Eq.(9) with V_{sm}
Arm inductance (L_{arm})	28 mH	Initial parameter from Eq.(11) (X_{Lpu} = 0.1 [p.u] and I_{2f} = 0.3 [kA])
SM capacitance (C_{sm})	6000 μF	Initial parameter from Eq.(10) (EP_0 = 50 [kJ/MVA])
Maximum allowable modulation index (m_{max})	0.85	From Eq.(20)
Individual SM voltage (V_{sm})	2.4 kV	Arbitrary voltage rating = 4 [kV] and λ_v is 60 [%]
Arm current (I_{arm})	973.9 A	From Eq.(30)
Capacitor voltage ripple factor (k_{max})	$\pm$5%	Arbitrary voltage ripple requirement

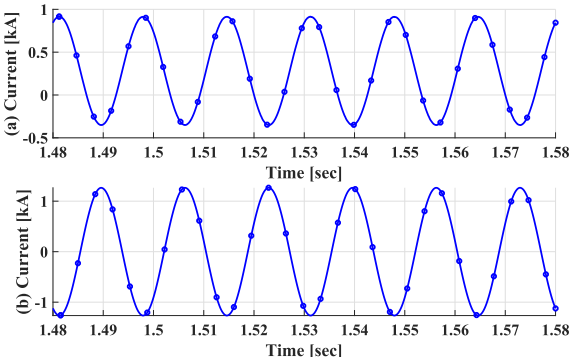

FIGURE 8. Simulation results: (a) arm current and (b) AC current.

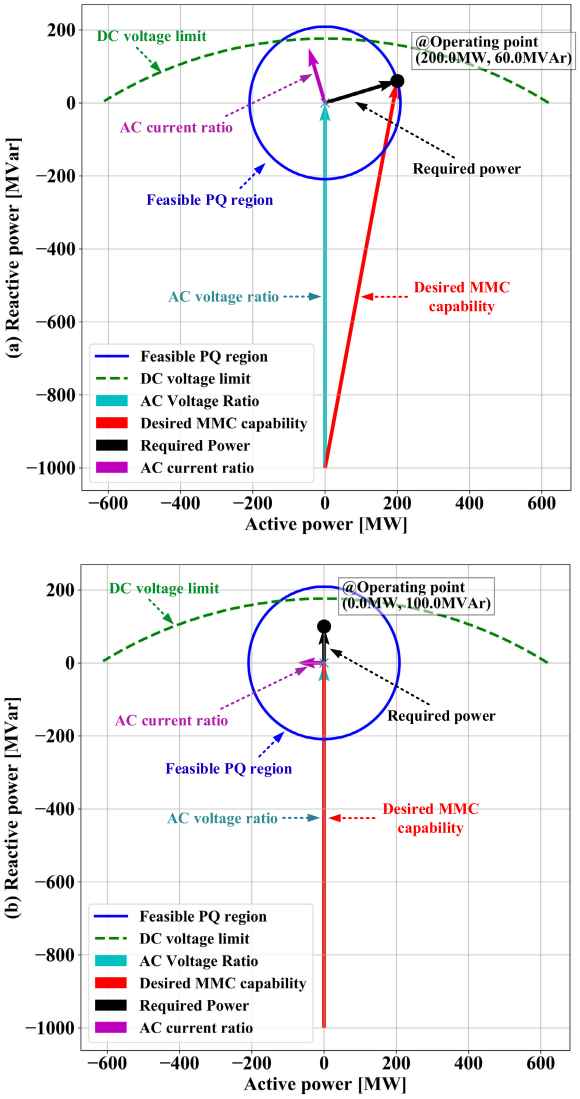

FIGURE 9. Simulation results: PQ capability: (a) normal operation for a required HVDC system and (b) STATCOM mode for grid support.

B. REAL-TIME DIGITAL SIMULATION (RTDS) RESULTS BASED ON HARDWARE-IN-LOOP SYSTEM (HILS)

An experimentation based on real-time digital simulator with hardware-in-loop system is performed for validation of proposed design methodology. The RTDS system consists of Giga Transceiver Workstation InterFace (GTWIF) and PB5 processor cards mounted on main rack, and Xilinx ML-605 FPGA board for the MMC-FPGA Unified Model (U5) control and operation, which is shown in Fig. 11 [59], [63], [64]. The MMC simulation model in the VSC bridge box of the RTDS is computed for 2.5 μsec, which is enough time for 512 SM capacitor voltages to transfer between ML-605 and the customized physical controller based on Xilinx's Aurora Protocol with 5.0 Gbps high speed serial communication. Sorting algorithm of 432 capacitor voltages can be completed in only 434 clocks; the operation clock was set to 200 MHz (5 nsec per clock). RTDS and HILS can be synchronized by the Grand Master Clock (GMC) as in [64]. The customized physical controller operates every time at 10 μsec for a control period.

Table 3 indicates the main parameter values obtained from the proposed design method for verifying the efficacy in a similar way of PSCAD/EMTDC simulation. Fig. 12 shows the HILS-based experimental results to verify the model of the required MMC-HVDC system. Fig. 12(a) shows the active and reactive power that are 800 MW and 80 MVar, respectively. The value of 800 MW and 80 MVar (capacitive mode) can be transformed to the value of $\pm$5 V scale in the RTDS based HILS testing, since a scaling factor is adopted due to a limited range of peak value for D/A output (it is possible to $\pm$10 V, but $\pm$5 V is selected to prevent an overstretch for the measured data) defined by Giga-Transceiver Analog Output (GTAO) card in RTDS [65]. Figs. 12(b), (c) and (d) are AC voltage/current at rectifier side and short term AC voltage/current of (b), and DC voltage/current, respectively,

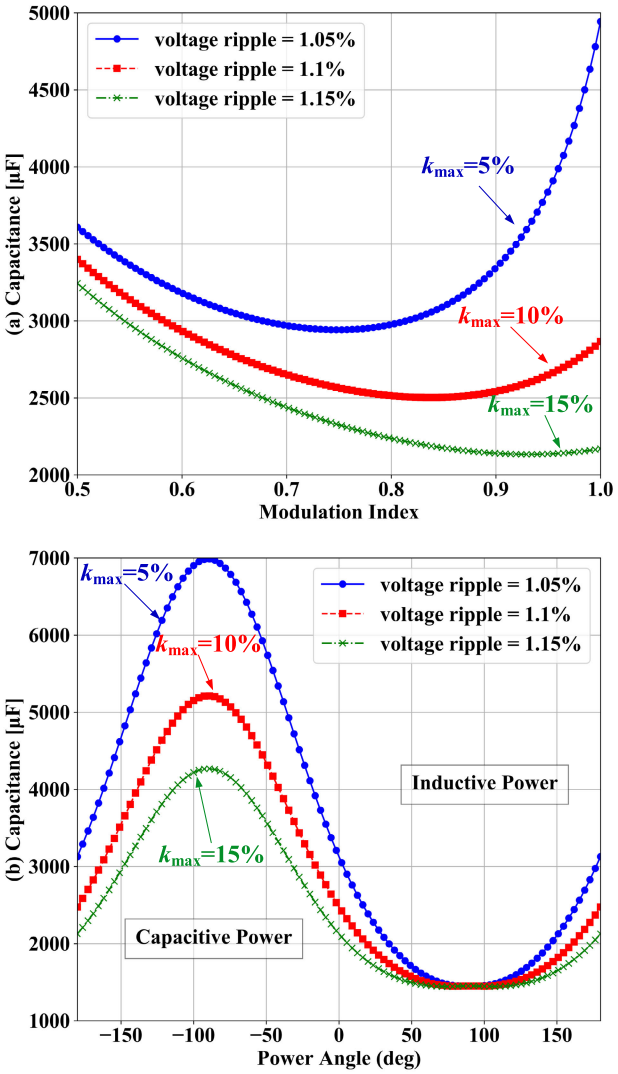

FIGURE 10. Simulation results: SM capacitance associated with (a) modulation index and (b) power angle.

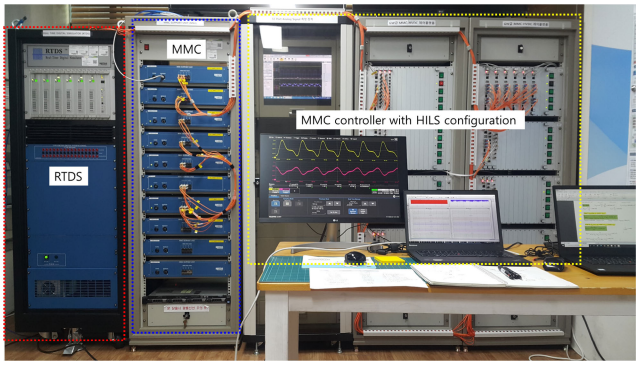

FIGURE 11. Hardware-in-Loop System (HILS) Configuration with MMC controller.

which are identically applied with a scaling factor as depicted in Fig. 12(a). The MMC-HVDC system is identically configured in the RTDS as Fig. 2. Especially, the MMC station 2

TABLE 3. MMC-HVDC system parameters for RTDS-HILS system.

Parameter	Value	Description
Active power (P_s)	800 MW	Required value at steady state
Reactive power (Q_s)	80 MVar	Desired value for AC voltage control at point of connection (POC)
System frequency	60 Hz	Fundamental frequency
Transformer voltage @ grid side (V_s)	915.98 kV	Defined value
Transformer voltage @ valve side (V_c)	423.89 kV	For stable operation of MMC from Eq.(20) and Eq.(22)
DC voltage (V_{dc})	±400 kV	Estimated value without economical requirement
DC current (I_{dc})	1000 A	No consideration of DC cable distance
No. of SMs (N_0)	432 ea	From Eq.(9) with V_{sm}
Arm inductance (L_{arm})	87.865 mH	Initial parameter from Eq.(11) (X_{Lpu} = 0.1 [p.u] and I_{2f} = 0.3 [kA])
SM capacitance (C_{sm})	9275 μF	Initial parameter from Eq.(10) (EP_0 = 50 [kJ/MVA])
Maximum allowable modulation index (m_{max})	0.865	From Eq.(20)
Individual SM voltage (V_{sm})	1.85 kV	Arbitrary voltage rating = 3 [kV] and λ_v is 60 [%]
Arm current (I_{arm})	1.128 A	From Eq.(30)
Capacitor voltage ripple factor (k_{max})	±5%	Arbitrary voltage ripple requirement

(rectifier mode) is applied with the step 8 for final MAMI adding to the compensation signal obtained from the step 5. On the other hand, in case of MMC Station 1 (inverter mode), MAMI is not applied which is also the result of EMTDC simulation; consequently, we may notice that the application of MAMI indicates the improved performance as in Fig. 7.

Therefore, Fig. 13 shows the experimental results of the capacitor voltage ripple and arm current. As shown in Fig. 13(a), the capacitor voltage in the inverter side without proposed method has the voltage ripple factor as 8 %; on the other hand, the rectifier side with proposed method has 3.35 % as an anticipated result. As shown in Fig. 13(b), the peak value of arm current calculated by (30) is 1.128 kA, while γ_0 is 1.128 and I_{dc} is 1000 A. Fig. 14 shows the experimental results regarding the MAMI. As mentioned above, both waveforms depicted in Fig. 14(a) as Initial and Final MAMI depends on the CCSC, resulting in the improvement of arm current in Final MAMI as shown in Fig. 13(b). For more detailed validation, the zoom-in waveform in Fig. 14(b) has a distinction in the MAMI. The distinct voltage is 95 mV (0.019 obtained from (21)) between 4.685 V(MAMI=0.937) at rectifier side and 4.590 (MAMI=0.918) at inverter side.

C. REVIEW OF DETERMINED PARAMETERS

Table 2 shows the verified parameters obtained from the proposed systematic design procedure without an iterated optimization process. As mentioned above, economic and reliability evaluations are required to obtain the final parameters for an optimized MMC-HVDC system. The remaining procedure is as follows:

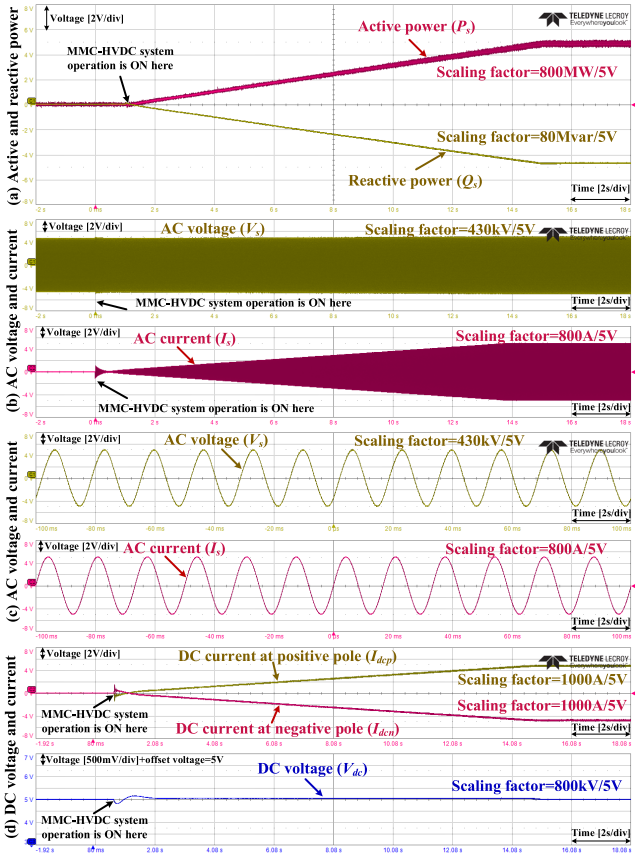

FIGURE 12. Experimental results: (a) active and reactive power, (b) AC voltage and current, (c) short-term AC voltage and current (Zoom-in of (b)), and (d) DC current and voltage.

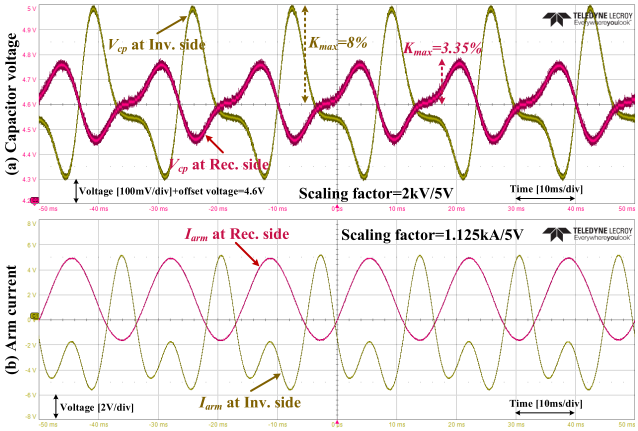

FIGURE 13. Experimental results: (a) capacitor voltage and (b) arm current.

- Economical evaluation for DC voltage that determines insulators and the number of the switching device through a process of the design step (Step 2) with Fig. 4
- Economical evaluation for DC current that determines the cost of long-distance DC cable and the number of switching devices

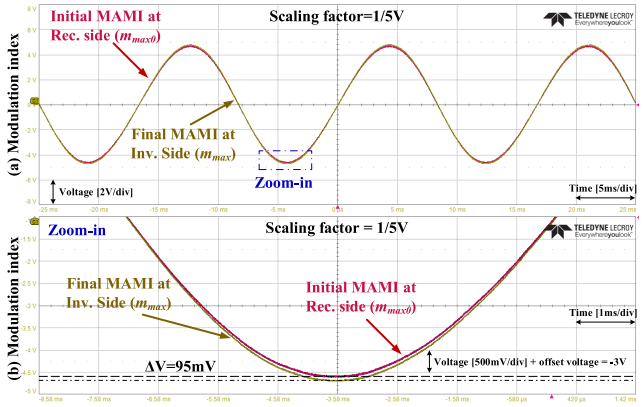

FIGURE 14. Experimental results: (a) modulation index and (b) modulation index (zoom-in).

- Economical and reliability evaluations for arm inductance that determines fault current rising rate relating to turn-off time delay of the switching device to protect the MMC-HVDC system and analysis of the reactive power loss
- Economical evaluations for SM capacitance that determines the voltage ripple affecting the switching frequency in terms of power conversion loss with the $k_{\max}$ through Fig. 10 based on [26].
- Economical evaluations for IGBT current rating considering the cost of commercial products.

VI. CONCLUSION

This study analyzed the coupled relationship between HVDC system and MMC, and proposed a systematic design procedure for determining the parameters of the MMC-HVDC system. The inspection is conducted to discover the relationship between control algorithms and the parameters, and the validated results are presented through PSCAD/EMTDC time-domain simulations and RTDS based HILS testing. The optimization process to finalize the complete parameters for the MMC-HVDC system was not included. However, this research could provide researchers with a superior design approach to extend their high technology challenges, and expands the MMC-HVDC based future DC grid.

REFERENCES

[1] A. Lesnicar and R. Marquardt, "An innovative modular multilevel converter topology suitable for a wide power range," in *Proc. IEEE Bologna Power Tech Conf.*, vol. 3, Jun. 2003, p. 6.
[2] M. Glinka and R. Marquardt, "A new AC/AC-multilevel converter family applied to a single-phase converter," in *Proc. 5th Int. Conf. Power Electron. Drive Syst. (PEDS)*, vol. 1, Nov. 2003, pp. 16–23.
[3] B. Gemmell, J. Dorn, D. Retzmann, and D. Soerangr, "Prospects of multilevel VSC technologies for power transmission," in *Proc. IEEE/PES Transmiss. Distribution Conf. Expo.*, Apr. 2008, pp. 1–16.
[4] R. Marquardt and A. Lesnicar, "New concept for high voltage modular multilevel converter," in *Proc. PESC Conf. Aachen*, 2004.
[5] J. Dorn, H. Huang, and D. Retzmann, "A new multilevel voltage-sourced converter topology for HVDC applications," in *Proc. CIGRE Session B4-304*, 2008, pp. 1–8.
[6] R. H. Renner and D. Van Hertem, "Ancillary services in electric power systems with HVDC grids," *IET Gener., Transmiss. Distrib.*, vol. 9, no. 11, pp. 1179–1185, Aug. 2015.

[7] D. Gamboa, "Control of MMC in HVDC applications," M.S. thesis, Dept. Energy Technol., Aalborg Univ., Aalborg, Denmark, 2013. [Online]. Available: https://projekter.aau.dk/projekter/files/76920132/Control of MMC in HVDC Applications Masters Thesis WPS4 1054.pdf

[8] R. H. Renner and D. V. Hertem, "Potential of using DC voltage restoration reserve for HVDC grids," *Electr. Power Syst. Res.*, vol. 134, pp. 167–175, May 2016. [Online]. Available: http://www.sciencedirect.com/science/article/pii/S0378779616000092

[9] A. Antonopoulos, L. Angquist, S. Norrga, K. Ilves, L. Harnefors, and H.-P. Nee, "Modular multilevel converter AC motor drives with constant torque from zero to nominal speed," *IEEE Trans. Ind. Appl.*, vol. 50, no. 3, pp. 1982–1993, May 2014.

[10] A. Antonopoulos, K. Ilves, L. Angquist, and H.-P. Nee, "On interaction between internal converter dynamics and current control of high-performance high-power AC motor drives with modular multilevel converters," in *Proc. IEEE Energy Convers. Congr. Expo.*, Sep. 2010, pp. 4293–4298.

[11] S. Debnath, J. Qin, B. Bahrani, M. Saeedifard, and P. Barbosa, "Operation, control, and applications of the modular multilevel converter: A review," *IEEE Trans. Power Electron.*, vol. 30, no. 1, pp. 37–53, Jan. 2015.

[12] Q. Song, W. Liu, X. Li, H. Rao, S. Xu, and L. Li, "A steady-state analysis method for a modular multilevel converter," *IEEE Trans. Power Electron.*, vol. 28, no. 8, pp. 3702–3713, Aug. 2013.

[13] H. Saad, X. Guillaud, J. Mahseredjian, S. Dennetiere, and S. Nguefeu, "MMC capacitor voltage decoupling and balancing controls," *IEEE Trans. Power Del.*, vol. 30, no. 2, pp. 704–712, Apr. 2015.

[14] A. Antonopoulos, L. Angquist, and H.-P. Nee, "On dynamics and voltage control of the modular multilevel converter," in *Proc. 13th Eur. Conf. Power Electron. Appl.*, Sep. 2009, pp. 1–10.

[15] S. Fan, K. Zhang, J. Xiong, and Y. Xue, "An improved control system for modular multilevel converters with new modulation strategy and voltage balancing control," *IEEE Trans. Power Electron.*, vol. 30, no. 1, pp. 358–371, Jan. 2015.

[16] L. Harnefors, A. Antonopoulos, S. Norrga, L. Angquist, and H.-P. Nee, "Dynamic analysis of modular multilevel converters," *IEEE Trans. Ind. Electron.*, vol. 60, no. 7, pp. 2526–2537, Jul. 2013.

[17] A. Antonopoulos, L. Angquist, L. Harnefors, K. Ilves, and H.-P. Nee, "Global asymptotic stability of modular multilevel converters," *IEEE Trans. Ind. Electron.*, vol. 61, no. 2, pp. 603–612, Feb. 2014.

[18] L. Angquist, A. Antonopoulos, D. Siemaszko, K. Ilves, M. Vasiladiotis, and H.-P. Nee, "Inner control of modular multilevel Converters–An approach using open-loop estimation of stored energy," in *Proc. Int. Power Electron. Conf. (ECCE ASIA)*, Jun. 2010, pp. 1579–1585.

[19] L. Angquist, A. Antonopoulos, D. Siemaszko, K. Ilves, M. Vasiladiotis, and H.-P. Nee, "Open-loop control of modular multilevel converters using estimation of stored energy," *IEEE Trans. Ind. Appl.*, vol. 47, no. 6, pp. 2516–2524, Nov. 2011.

[20] K. Ilves, A. Antonopoulos, S. Norrga, and H.-P. Nee, "Steady-state analysis of interaction between harmonic components of arm and line quantities of modular multilevel converters," *IEEE Trans. Power Electron.*, vol. 27, no. 1, pp. 57–68, Jan. 2012.

[21] S. Cui and S.-K. Sul, "A comprehensive DC short-circuit fault ride through strategy of hybrid modular multilevel converters (MMCs) for overhead line transmission," *IEEE Trans. Power Electron.*, vol. 31, no. 11, pp. 7780–7796, Nov. 2016.

[22] R. Marquardt, "A new modular voltage source inverter topology," in *Proc. Conf. Rec. EPE*, 2003. [Online]. Available: https://ci.nii.ac.jp/naid/10027637272/en/

[23] G. Ding, M. Ding, and G. Tang, "An innovative modular multilevel converter topology and modulation control scheme for the first VSC-HVDC project in China," in *16th PSCC Glasgow Scotland*, Jul. 2008, pp. 1–8.

[24] E. P. Eni, "Fault tolerant distributed control strategy for modular multilevel converter in HVDC applications," M.S. thesis, Dept. Energy Technol., Aalborg Univ., Aalborg, Denmark, 2013. [Online]. Available: https://projekter.aau.dk/projekter/files/77496203/fault tolerant distributed control strategy for MMC in HVDC applications.pdf

[25] M. Eremia, J. A. Jardini, G. Tang, and L. Toma, *Advanced Solutions in Power Systems: HVDC, FACTS, and Artificial Intelligence*. Hoboken, NJ, USA: Wiley, 2016. [Online]. Available: https://onlinelibrary.wiley.com/doi/abs/10.1002/9781119175391.ch4

[26] K. Ilves, S. Norrga, L. Harnefors, and H.-P. Nee, "On energy storage requirements in modular multilevel converters," *IEEE Trans. Power Electron.*, vol. 29, no. 1, pp. 77–88, Jan. 2014.

[27] H. Barnklau, A. Gensior, and S. Bernet, "Submodule capacitor dimensioning for modular multilevel converters," *IEEE Trans. Ind. Appl.*, vol. 50, no. 3, pp. 1915–1923, May 2014.

[28] M. M. C. Merlin and T. C. Green, "Cell capacitor sizing in multilevel converters: Cases of the modular multilevel converter and alternate arm converter," *IET Power Electron.*, vol. 8, no. 3, pp. 350–360, Mar. 2015.

[29] M. M. C. Merlin, T. C. Green, P. D. Mitcheson, F. J. Moreno, K. J. Dyke, and D. R. Trainer, "Cell capacitor sizing in modular multilevel converters and hybrid topologies," in *Proc. 16th Eur. Conf. Power Electron. Appl.*, Aug. 2014, pp. 1–10.

[30] B. Jacobson, P. Karlsson, G. Asplund, L. Harnefors, and T. Jonsson, "VSC-HVDC transmission with cascaded two-level converters," in *Proc. CIGRE Session B4-110*, 2008.

[31] M. Zygmanowski, B. Grzesik, and R. Nalepa, "Capacitance and inductance selection of the modular multilevel converter," in *Proc. 15th Eur. Conf. Power Electron. Appl. (EPE)*, Sep. 2013, pp. 1–10.

[32] D. Jovcic, "Multilevel VSC converters in HVDC applications," in *High Voltage Direct Current Transmission*. Hoboken, NJ, USA: Wiley, 2019, ch. 16, pp. 205–225. [Online]. Available: https://onlinelibrary.wiley.com/doi/abs/10.1002/9781119566632.ch16, doi: 10.1002/9781119566632.ch16.

[33] R. Wachal, A. Jindal, S. Dennetiere, H. Saad, and O. Rui, "Guide for the development of models for HVDC converters in a HVDC grid," CIGRE Working Group, Tech. Rep. TB 604, B4.57, Dec. 2014. [Online]. Available: http://e-Cigre.org

[34] Y. Tang, L. Ran, O. Alatise, and P. Mawby, "Capacitor selection for modular multilevel converter," *IEEE Trans. Ind. Appl.*, vol. 52, no. 4, pp. 3279–3293, Jul. 2016.

[35] B. Li, Z. Xu, S. Shi, D. Xu, and W. Wang, "Comparative study of the active and passive circulating current suppression methods for modular multilevel converters," *IEEE Trans. Power Electron.*, vol. 33, no. 3, pp. 1878–1883, Mar. 2018.

[36] K. Ilves, S. Norrga, L. Harnefors, and H.-P. Nee, "Analysis of arm current harmonics in modular multilevel converters with main-circuit filters," in *Proc. Int. Multi-Conf. Syst., Sygnals Devices*, Mar. 2012, pp. 1–6.

[37] K. Shen, S. Wang, D. Zhao, and G. Zhao, "Influence of two-stage coupled arm inductors on modular multilevel converter," *IEEE Access*, vol. 7, pp. 162488–162499, 2019.

[38] T. Li, A. M. Gole, and C. Zhao, "Harmonic instability in MMC-HVDC converters resulting from internal dynamics," *IEEE Trans. Power Del.*, vol. 31, no. 4, pp. 1738–1747, Aug. 2016.

[39] Q. Tu, Z. Xu, H. Huang, and J. Zhang, "Parameter design principle of the arm inductor in modular multilevel converter based HVDC," in *Proc. Int. Conf. Power Syst. Technol.*, Oct. 2010, pp. 1–6.

[40] Y. Li, X. Shi, B. Liu, F. Wang, and W. Lei, "Maximum modulation index for modular multilevel converter with circulating current control," in *Proc. IEEE Energy Convers. Congr. Expo. (ECCE)*, Sep. 2014, pp. 491–498.

[41] S. Sim, C. Kim, and J. Kang, "Optimal design method for maximum modulation index of VSC HVDC based on MMC considering compensation signals and AC network conditions," in *Proc. 10th Int. Conf. Power Electron. ECCE Asia (ICPE-ECCE Asia)*, May 2019, pp. 3235–3239.

[42] P. D. Judge, G. Chaffey, M. M. C. Merlin, P. R. Clemow, and T. C. Green, "Dimensioning and modulation index selection for the hybrid modular multilevel converter," *IEEE Trans. Power Electron.*, vol. 33, no. 5, pp. 3837–3851, May 2018.

[43] C. Oates, "Modular multilevel converter design for VSC HVDC applications," *IEEE J. Emerg. Sel. Topics Power Electron.*, vol. 3, no. 2, pp. 505–515, Jun. 2015.

[44] Z. Xu, H. Xiao, and Z. Zhang, "Selection methods of main circuit parameters for modular multilevel converters," *IET Renew. Power Gener.*, vol. 10, no. 6, pp. 788–797, Jul. 2016.

[45] Y. Sun, C. A. Teixeira, D. G. Holmes, B. P. McGrath, and J. Zhao, "Low-order circulating current suppression of PWM-based modular multilevel converters using DC-link voltage compensation," *IEEE Trans. Power Electron.*, vol. 33, no. 1, pp. 210–225, Jan. 2018.

[46] Q. Tu, Z. Xu, and L. Xu, "Reduced switching-frequency modulation and circulating current suppression for modular multilevel converters," *IEEE Trans. Power Del.*, vol. 26, no. 3, pp. 2009–2017, Jul. 2011.

[47] D. Siemaszko, "Fast sorting method for balancing capacitor voltages in modular multilevel converters," *IEEE Trans. Power Electron.*, vol. 30, no. 1, pp. 463–470, Jan. 2015.

[48] A. Hassanpoor, L. Angquist, S. Norrga, K. Ilves, and H.-P. Nee, "Tolerance band modulation methods for modular multilevel converters," *IEEE Trans. Power Electron.*, vol. 30, no. 1, pp. 311–326, Jan. 2015.

[49] J. Qin and M. Saeedifard, "Reduced switching-frequency voltage-balancing strategies for modular multilevel HVDC converters," *IEEE Trans. Power Del.*, vol. 28, no. 4, pp. 2403–2410, Oct. 2013.
[50] P. M. Meshram and V. B. Borghate, "A simplified nearest level control (NLC) voltage balancing method for modular multilevel converter (MMC)," *IEEE Trans. Power Electron.*, vol. 30, no. 1, pp. 450–462, Jan. 2015.
[51] M. Abdelsalam, M. Marei, S. Tennakoon, and A. Griffiths, "Capacitor voltage balancing strategy based on sub-module capacitor voltage estimation for modular multilevel converters," *CSEE J. Power Energy Syst.*, vol. 2, no. 1, pp. 65–73, Mar. 2016.
[52] J. Pou, S. Ceballos, G. Konstantinou, V. G. Agelidis, R. Picas, and J. Zaragoza, "Circulating current injection methods based on instantaneous information for the modular multilevel converter," *IEEE Trans. Ind. Electron.*, vol. 62, no. 2, pp. 777–788, Feb. 2015.
[53] K. Ilves, A. Antonopoulos, S. Norrga, and H.-P. Nee, "A new modulation method for the modular multilevel converter allowing fundamental switching frequency," *IEEE Trans. Power Electron.*, vol. 27, no. 8, pp. 3482–3494, Aug. 2012.
[54] Y. Xu, Z. Xu, Z. Zhang, and H. Xiao, "A novel circulating current controller for MMC capacitor voltage fluctuation suppression," *IEEE Access*, vol. 7, pp. 120141–120151, 2019.
[55] J.-J. Jung, S. Cui, Y. Lee, and S.-K. Sul, "A cell capacitor energy balancing control of MMC-HVDC under the AC grid faults," in *Proc. 9th Int. Conf. Power Electron. ECCE Asia (ICPE-ECCE Asia)*, Jun. 2015, pp. 1–8.
[56] A. Hassanpoor, K. Ilves, S. Norrga, L. Angquist, and H.-P. Nee, "Tolerance-band modulation methods for modular multilevel converters," in *Proc. 15th Eur. Conf. Power Electron. Appl. (EPE)*, Sep. 2013, pp. 1–10.
[57] J. Kang, H. Kim, H.-J. Jung, D.-S. Lee, C.-K. Kim, H. A. Mantooth, and K. Hur, "On exploiting active redundancy of a modular multilevel converter to balance reliability and operational flexibility," *IEEE Trans. Power Electron.*, vol. 34, no. 3, pp. 2234–2243, Mar. 2019.
[58] K. Ilves, A. Antonopoulos, S. Norrga, L. Ängquist, and H. Nee, "Controlling the ac-side voltage waveform in a modular multilevel converter with low energy-storage capability," in *Proc. 14th Eur. Conf. Power Electron. Appl.*, Aug./Sep. 2011, pp. 1–8.
[59] J. Lee, D. Kang, and J. Lee, "A study on the improved capacitor voltage balancing method for modular multilevel converter based on Hardware-In-the-Loop simulation," *Electronics*, vol. 8, no. 10, p. 1070, Sep. 2019.
[60] T. Nam, H. Kim, S. Kim, G. T. Son, Y.-H. Chung, J.-W. Park, C.-K. Kim, and K. Hur, "Trade-off strategies in designing capacitor voltage balancing schemes for modular multilevel converter HVDC," *J. Electr. Eng. Technol.*, vol. 11, no. 4, pp. 829–838, Jul. 2016.
[61] J. Xu, C. Zhao, Y. Xiong, C. Li, Y. Ji, and T. An, "Optimal design of MMC levels for electromagnetic transient studies of MMC-HVDC," *IEEE Trans. Power Del.*, vol. 31, no. 4, pp. 1663–1672, Aug. 2016.
[62] H. Saad, T. Ould-Bachir, J. Mahseredjian, C. Dufour, S. Dennetiere, and S. Nguefeu, "Real-time simulation of MMCs using CPU and FPGA," *IEEE Trans. Power Electron.*, vol. 30, no. 1, pp. 259–267, Jan. 2015.
[63] T. Maguire, B. Warkentin, Y. Chen, and J. Hasler, "Efficient techniques for real time simulation of MMC systems," in *Proc. Int. Conf. Power Syst. Transients (IPST)*, 2013, pp. 1–7.
[64] J. Lee, J. Park, D. Kang, D. Yoo, and J. J. Lee, "Comparison of capacitor voltage balancing methods for 1GW MMC-HVDC based on real-time digital simulator and physical control systems," *J. Power Electron.*, vol. 19, no. 5, pp. 1171–1181, 2019.
[65] V. Pagola, R. Peña, J. Segundo, and A. Ospino, "Rapid prototyping of a hybrid PV–Wind generation system implemented in a real-time digital simulation platform and arduino," *Electronics*, vol. 8, no. 1, p. 102, Jan. 2019.

JAESIK KANG (Member, IEEE) received the M.S. and Ph.D. degrees in electrical and electronic engineering from Yonsei University, Seoul, South Korea, in 2013 and 2019, respectively. He was a Research and Development Engineer with the Korea Railroad Research Institute (KRRI), Uiwang, South Korea, in 2013. He was with LG Display, Paju, South Korea, in 2014. Since 2019, he has been joined the Korea Electrotechnology Research Institute (KERI), Changwon, South Korea. His research interests include modeling and control of power converters, modular multilevel converters, flexible ac transmission systems/high-voltage direct current, and power electronic applications in power systems.

DAE-WOOK KANG (Member, IEEE) received the B.S., M.S., and Ph.D. degrees in electrical engineering from Hanyang University, Seoul, South Korea, in 1998, 2000, and 2004, respectively. Since 2004, he has been joined the Korea Electrotechnology Research Institute (KERI), Changwon, South Korea. His current interests include HVDC/MVDC, MTDC, ESS, renewable energy, and the applications of power electronics based on multilevel converter.

JONG-PIL LEE (Member, IEEE) received the B.S. degree in control and instrumentation of engineering and the M.S. degree in electrical engineering from Korea University, South Korea, in 1997 and 1999, respectively, and the Ph.D. degree from the School of Electrical Engineering, Korea University, in 2012. From 1999 to 2005, he was a Senior Researcher with the Department of Electric and Hybrid Vehicle Research, Hyundai Heavy Industries. From 2006 to 2013, he worked as a Senior Researcher with the Power Electric Research Group, Korea Electrotechnology Research Institute (KERI), South Korea. Since 2018, he has been working as the Director of the Power Conversion System Research Center, KERI. From 2015 to 2018, he worked as a Professor with the Energy and Power Conversion Engineering, University of Science and Technology (UST). Since 2019, he has also been working as a Member of the Board of Director of the Korea Institute of Power Electronics. His main research interests include grid-connected PCS for renewable power source, smart energy storage system PCS, distributed power generation systems, and power conversion for HVDC, MVDC, and LVDC systems.

DONG WOOK YOO (Member, IEEE) received the B.S. degree in electrical engineering from Sungkyunkwan University (SKKU), Suwon, South Korea, in 1983, the M.S. degree in electrical engineering from Yonsei University, Seoul, South Korea, in 1985, and the Ph.D. degree in power electronics from SKKU, in 1997. He is currently working with the Korea Electrotechnology Research Institute (KERI), Changwon, South Korea, where he became a Researcher in 1985, a Senior Researcher in 1989, and a Principal Researcher in 1997. Since 1997, he has been a Team Leader with the Power Electronics Laboratory, the Renewable Energy Laboratory, and the Power Conversion Control Research Center, KERI. In addition, he is an Executive Director with the HVDC Research Division, KERI. He is also serving as a Vice President of KERI. He is a member of the IEEE Power Electronics Society, the IEEE Industry Applications Society, the Korean Institute of Power Electronics (KIPE), and the Korean Institute of Electrical Engineers (KIEE). He was a Committee Member of KIEE from 2005 to 2006, and of KIPE from 2009 to 2010, and he served as the President of KIPE in 2017. He is currently the Director of Direct Current Power Transmission & Distribution System Initiative at the Ministry of Trade Industry & Energy of Korea. He was a co-recipient of a Best Paper Award at the 2002 Annual Conference of the IEEE Industrial Electronics Society, and a Best Paper Award at the 2007 International Conference on Power Electronics, Daegu, South Korea. In 2009, he became the Chairman of a KIPE Conference.

JAE WOONG SHIM (Member, IEEE) received the Ph.D. degree in electrical engineering from Yonsei University, Seoul, South Korea, and The University of Sydney, Sydney, NSW, Australia, in 2016. He was a Senior Researcher with the HVDC Research Center, LS Electric, from 2016 to 2017, for FACTS/HVDC operation and control. He has been with the Department of Energy Engineering, Inje University, South Korea, since 2017. His research interests include power system dynamics and control, HVDC/FACTS/ESS operation, multi-terminal HVDC/MVDC, integration of renewable energy sources, and the interfaces of power electronics devices on power systems.